

# MHC Dextramer<sup>®</sup> – Detect with Confidence

Get the full picture of **CD8+** and **CD4+** T-cell responses  
Even the low-affinity ones  
Available also in GMP



**immuDEX**  
PRECISION IMMUNE MONITORING

## The Journal of Immunology

RESEARCH ARTICLE | DECEMBER 01 1999

### Urokinase Receptor (CD87) Aggregation Triggers Phosphoinositide Hydrolysis and Intracellular Calcium Mobilization in Mononuclear Phagocytes<sup>1</sup> **FREE**

Robert G. Sitrin; ... et. al

*J Immunol* (1999) 163 (11): 6193–6200.

<https://doi.org/10.4049/jimmunol.163.11.6193>

#### Related Content

Clustering of Urokinase Receptors (uPAR; CD87) Induces Proinflammatory Signaling in Human Polymorphonuclear Neutrophils

*J Immunol* (September,2000)

Cutting Edge: Evidence for a Signaling Partnership Between Urokinase Receptors (CD87) and L-Selectin (CD62L) in Human Polymorphonuclear Neutrophils

*J Immunol* (April,2001)

Urokinase Receptor-Deficient Mice Have Impaired Neutrophil Recruitment in Response to Pulmonary *Pseudomonas aeruginosa* Infection

*J Immunol* (August,2000)

# Urokinase Receptor (CD87) Aggregation Triggers Phosphoinositide Hydrolysis and Intracellular Calcium Mobilization in Mononuclear Phagocytes<sup>1</sup>

Robert G. Sitrin,<sup>2\*</sup> Pauline M. Pan,<sup>\*</sup> Hollie A. Harper,<sup>\*</sup> R. Alexander Blackwood,<sup>†</sup> and Robert F. Todd III<sup>‡</sup>

Leukocytes utilize urokinase receptors (uPAR; CD87) in adhesion, migration, and matrix proteolysis. uPAR aggregate at cell-substratum interfaces and at leading edges of migrating cells, so this study was undertaken to determine whether uPAR aggregation is capable of initiating activation signaling. Monocyte-like U937 cells were labeled with fluo-3-acetoxymethyl ester to quantitate intracellular  $\text{Ca}^{2+}$  concentrations ( $[\text{Ca}^{2+}]_i$ ) by spectrofluorometry, and uPAR was aggregated by mAb cross-linking. uPAR aggregation induced highly reproducible increases in  $[\text{Ca}^{2+}]_i$  of  $103.0 \pm 10.9$  nM ( $p < 0.0001$ ) and >3-fold increases in cellular *d*-myoinositol 1,4,5-trisphosphate (Ins(1,4,5) $\text{P}_3$ ) levels. Similar increases in  $[\text{Ca}^{2+}]_i$  were also elicited by uPAR aggregation in human monocytes, but cross-linking a control IgG2a had no effect on  $[\text{Ca}^{2+}]_i$ . Selectively cross-linking uPA-occupied uPAR with an anti-uPA mAb produced smaller increases in  $[\text{Ca}^{2+}]_i$ , but fully saturating uPAR with exogenous uPA enhanced the  $[\text{Ca}^{2+}]_i$  response to equal the effect of aggregating uPAR directly. Increased  $[\text{Ca}^{2+}]_i$  was inhibited by thapsigargin, herbimycin A, and U73122, but only partially reduced by low extracellular  $[\text{Ca}^{2+}]_o$ , indicating that uPAR aggregation increases  $[\text{Ca}^{2+}]_i$  by activating phospholipase C through a tyrosine kinase-dependent mechanism, generating Ins(1,4,5) $\text{P}_3$  and releasing  $\text{Ca}^{2+}$  from Ins(1,4,5) $\text{P}_3$ -sensitive intracellular stores. Cross-linking the  $\beta_2$  integrin CR3 could not duplicate the effect of uPAR cross-linking, and uPAR-triggered  $\text{Ca}^{2+}$  mobilization was not blocked by anti-CR3 mAbs. These results indicate that uPAR aggregation initiates phosphoinositide hydrolysis by mechanisms that are not strictly dependent on associated uPA or CR3. *The Journal of Immunology*, 1999, 163: 6193–6200.

Leukocytes progress through a complex series of transitions as they are recruited into sites of inflammation. In many circumstances, cellular adhesion through L-selectin and  $\beta_2$  integrins will initiate the process, followed by directional migration across cellular and stromal barriers (1). Activation to a proinflammatory phenotype often overlaps with the process of recruitment, and the mechanisms by which activation is coupled to cellular migration has been the subject of considerable investigation. Prior work has demonstrated that uPAR<sup>3</sup> (CD87), the plasma membrane receptor for urokinase plasminogen activator (uPA), serves many important functions in leukocyte adhesion and movement (2–7). uPAR complexes with  $\beta_1$  and  $\beta_2$  integrins, in some instances modulating the adhesive functions of these proteins (5–8). Originally, it was generally held that the primary function of uPAR on the plasma membrane is to concentrate uPA catalytic activity near the cell surface, efficiently activating pericellular

plasminogen to plasmin. The plasmin in turn would digest extracellular matrix proteins, facilitating cellular penetration through stromal barriers (2, 9). More recent work has shown that uPAR expression is also necessary for chemotaxis of human monocytes and neutrophils in vitro, and this function is not dependent on associated uPA (4, 10). There is considerable evidence that uPAR is also involved in activation signaling of leukocytes and other cells. uPAR colocalizes with a variety of proteins that participate in activation signaling, including *src* and Jak family tyrosine kinases (TKs), integrins, and cytoskeletal proteins (11–15). Binding uPA to uPAR can activate several signaling pathways and trigger complex effector functions such as proliferation, adhesion, and movement (11, 16–24). The concept that uPAR functions in activation signaling is appealing, in that it provides another mechanistic link between leukocyte recruitment and activation. Nonetheless, activation signaling through uPAR poses several problems. First, uPAR is a GPI-anchored protein, and as such has no direct conduit to signaling elements inside the cell (25). This could be circumvented by uPAR using other proteins as signal transduction devices, and precisely this mechanism has been demonstrated for uPA-induced  $\text{Ca}^{2+}$  fluxes in neutrophils, in which CR3 (Mac-1; CD11b/CD18), a  $\beta_2$  integrin, serves as the partner protein (8). Second, high concentrations of uPA, far exceeding the 0.1–0.5 nM  $K_d$  reported for uPAR (2), are often necessary to trigger signaling events. Unstimulated monocytes (26) and monocyte-like U937 cells (27) express uPAR that are approximately 50% occupied with uPA, while neutrophils reportedly express a lower proportion of occupied uPAR (28). With stimulation, changes in the occupancy rate are modest, and thus may not pertain to rapid changes in leukocyte function during recruitment (27). As cells adhere and migrate, one well-documented and characteristic change in uPAR

<sup>\*</sup>Pulmonary and Critical Care Medicine Division, <sup>‡</sup>Hematology/Oncology Division, Department of Internal Medicine, and <sup>†</sup>Department of Pediatrics and Communicable Diseases, University of Michigan, Ann Arbor, MI 48109

Received for publication July 6, 1999. Accepted for publication September 21, 1999.

The costs of publication of this article were defrayed in part by the payment of page charges. This article must therefore be hereby marked *advertisement* in accordance with 18 U.S.C. Section 1734 solely to indicate this fact.

<sup>1</sup> This work was supported by National Institutes of Health Grants HL53283 (R.G.S.), AI35877 (R.A.B.), and CA 42246 and CA39064 (R.F.T.).

<sup>2</sup> Address correspondence and reprint requests to Dr. Robert G. Sitrin, 6301 MSRB III, Box 0642, 1500 West Medical Center Drive, Ann Arbor, MI 48109-0642. E-mail address: rsitrin@umich.edu

<sup>3</sup> Abbreviations used in this paper: uPAR, urokinase plasminogen activator receptor;  $[\text{Ca}^{2+}]_i$ , intracellular  $\text{Ca}^{2+}$  concentration; fluo-3-AM, fluo-3-acetoxymethyl ester; HMW-uPA, high m.w. uPA; Ins(1,4,5) $\text{P}_3$ , *d*-myoinositol 1,4,5-trisphosphate; LTB<sub>4</sub>, leukotriene B<sub>4</sub>; TK, tyrosine kinase; uPA, urokinase plasminogen activator.

is aggregation at the cell-substratum interface, focal adhesions, and the leading edge of migration (4, 5, 29–31). Therefore, we speculated that uPAR aggregation could be an important triggering event that links cell adhesion and movement to activation signaling. In this study, we demonstrate that aggregating uPAR of U937 cells and human monocytes triggers  $[Ca^{2+}]_i$  mobilization by phosphoinositide hydrolysis.

## Materials and Methods

### Reagents

Purified Fc fragments of murine IgG and F(ab')<sub>2</sub> fragments of goat Ab reactive against murine IgG F(ab')<sub>2</sub> were obtained from Jackson ImmunoResearch Laboratories (West Grove, PA). The anti-uPAR mAb (IgG2a; clone 3B10) was purified by protein A affinity chromatography from mouse ascites and quantitated by protein content (32). The anti-β<sub>2</sub> integrin mAbs included anti-CD18 mAb (TS1/18; IgG1), anti-CD11b mAbs (clone 44 (IgG2a)), and clone OKM1 (IgG2b; American Type Culture Collection (ATCC), Manassas, VA), and were purified in similar fashion (33, 34). A mAb reactive to the human uPA catalytic domain and high m.w. uPA (HMW-uPA) were obtained from American Diagnostica, Greenwich, CT (catalogue 3940). Control IgG2a mAb was obtained from ICN Biomedicals (Costa Mesa, CA). Where indicated, mAb was biotinylated with sulfo-NHS-LC-biotin (Pierce, Rockford, IL). Streptavidin and herbimycin A were obtained from Sigma (St. Louis, MO).

### Cell purification and culture

The U937 monocytic leukemia cell line was obtained from the ATCC. Cells were propagated in 75-cm<sup>2</sup> polystyrene flasks in standard medium consisting of RPMI 1640 (Life Technologies, Grand Island, NY) with penicillin (100 U/ml), streptomycin (100 μg/ml), gentamicin (100 μg/ml), glutamine (2 mM), and 5% FBS (HyClone, Logan, UT). To purify human monocytes, peripheral blood was obtained from healthy volunteers according to the provisions of the University of Michigan Institutional Review Board for Human Subject Research. Anticoagulated blood was sedimented with 6% dextran in 0.9% NaCl, and the mononuclear cells were isolated by centrifugation over 10% Ficoll-Hypaque. The mononuclear cells were chilled, washed with PBS/1% BSA, filtered through 30-μm nylon mesh, and incubated with MACS CD14 Microbeads (Miltenyi Biotec, Auburn, CA) for 45 min at 4°C. The bead-coated cells were then positively selected by passage through VS<sup>+</sup> separation columns in the VarioMACS magnetic separation system (Miltenyi Biotec). Using this method, the cells obtained were >95% viable by trypan blue exclusion, and 95 ± 3% monocytes (mean ± SD), as determined by differential counting of Wright-Giemsa-stained cytocentrifuge preparations.

### Ab-mediated receptor cross-linking

Cells were preloaded with fluo-3-AM (see below), resuspended in experimental buffer (145 mM NaCl, 5 mM KCl, 1 mM MgCl<sub>2</sub>, 10 mM glucose, 1 mM CaCl<sub>2</sub>, 1% w/v BSA, 4 mM probenecid, 10 mM HEPES, pH 7.4). Unless indicated otherwise, cells were first incubated with murine IgG Fc fragments (150 μg/ml) at 4°C for 15 min to block binding of the primary Abs to FcR. Cells were then incubated with the primary Ab (12.5–25 μg/ml), as specified, at 4°C for 30 min, and finally, washed and resuspended in experimental buffer at 4°C. To initiate receptor cross-linking, F(ab')<sub>2</sub> fragments of goat anti-mouse F(ab')<sub>2</sub> Ab (100 μg/ml final concentration) were added after warming the cells to 37°C.

### Measurement of intracellular calcium

Cells (5 × 10<sup>6</sup>/ml) were loaded with the calcium-sensitive fluorescent dye fluo-3-AM (2 μM; Molecular Probes, Eugene, OR) at 30°C for 30 min in 145 mM NaCl, 5 mM KCl, 1 mM MgCl<sub>2</sub>, 10 mM glucose, 4 mM probenecid, and 10 mM HEPES, pH 7.4. After pretreatment with Abs, as indicated, 2.5 × 10<sup>6</sup> cells were suspended in a total of 1 ml incubation buffer and prewarmed to 37°C. Fluorescence intensity was then measured with a SLM8000 spectrofluorometer equipped with SLM Spectrum Processor version 3.5 software (SLM Instruments, Urbana, IL), using a 1-cm light path cuvette with continuous stirring at an excitation wavelength of 505 nm and an emission wavelength of 530 nm. Fluorescence measurements were acquired at 2-s intervals for 300 s. The fluorescence measurements were then converted to nanomolar concentrations of  $[Ca^{2+}]_i$  by the calibration method of Grynkiewicz et al. (35), using a  $K_d$  for fluo-3-AM of 864 nM (36).

### Measurement of d-myooinositol 1,4,5-trisphosphate (Ins(1,4,5)P<sub>3</sub>)

After cross-linking U937 cell uPAR, cells were extracted with 0.2 vol of perchloric acid at designated intervals. The extracts were pH adjusted with KOH and assayed for Ins(1,4,5)P<sub>3</sub> levels using a competitive binding assay according to the manufacturer's directions (Amersham Life Sciences, Arlington Heights, IL).

### Statistical analysis

Comparisons of group means were performed with two-tailed Student's *t* tests, with *p* values ≤ 0.05 deemed significant. Where indicated, multiple comparisons with a single control group were performed with Dunnett's test applied to one-way analysis of variance. All statistical analyses were performed with Prism version 2.0 software (Graph Pad Software, San Diego, CA).

## Results

### Ab-mediated uPAR cross-linking triggers increased $[Ca^{2+}]_i$

Fluo-3-AM-loaded U937 cells were treated with murine IgG Fc to block FcR, and subsequently treated with 12.5 μg/ml anti-uPAR mAb (3B10) or an equal concentration of isotype-matched IgG2a mAb. After introducing the cross-linking Ab to anti-uPAR-pretreated cells, there was a prompt and highly reproducible increase in  $[Ca^{2+}]_i$  (Fig. 1A). Because aggregation of receptors by Ab cross-linking is not an instantaneous process, there was an expected delay of 24.9 ± 1.8 s between addition of the cross-linking Ab and the onset of the increase in  $[Ca^{2+}]_i$ . The mean peak  $[Ca^{2+}]_i$  was double the baseline value, and the  $[Ca^{2+}]_i$  transient was sustained over 133.8 ± 5.2 s. By contrast, cross-linking the control IgG2a mAb produced no significant increase in  $[Ca^{2+}]_i$ . To further confirm that artifactual aggregation of FcR was not contributing to the increase in  $[Ca^{2+}]_i$ , the anti-uPAR mAb and the IgG2a control were cross-linked with and without prior blockade with murine Fc fragments (Fig. 1B). Cross-linking the IgG2a control mAb in the absence of FcR blockade produced a relatively small increase in  $[Ca^{2+}]_i$ . Blocking FcR completely abrogated this response, but had no effect at all on the increase in  $[Ca^{2+}]_i$  induced by cross-linking uPAR. The specificity of the uPAR cross-linking strategy was further demonstrated by using the competition between uPA and the 3B10 anti-uPAR mAb for binding to uPAR. Fully saturating uPAR with uPA decreases subsequent binding of the 3B10 mAb by 70% (37), in keeping with our own results (not shown). U937 cells were treated with HMW-uPA (1 μg/ml) before loading with anti-uPAR mAb, and the cross-linking protocol was completed as above. Prior uPA treatment decreased the resulting difference between baseline and peak  $[Ca^{2+}]_i$  ( $\Delta[Ca^{2+}]_i$ ) to 43.9 ± 4.5% of control (*p* = 0.01, *n* = 3). This effect was specific to uPAR cross-linking, since prior uPA treatment did not significantly affect the  $\Delta[Ca^{2+}]_i$  resulting from cross-linking the control IgG2a mAb in the absence of Fc blockade (121.5 ± 8.5% of control, *p* = NS). Binding uPA to uPAR had no direct effect on  $[Ca^{2+}]_i$ , independently of uPAR cross-linking (see below). Finally, preliminary experiments confirmed that  $[Ca^{2+}]_i$  did not change when cells were treated with either the anti-uPAR mAb or the cross-linking Ab alone (not shown).

To provide a frame of reference for the magnitude of  $[Ca^{2+}]_i$  mobilization induced by uPAR cross-linking, U937 cells were treated with LTB<sub>4</sub> (100 nM; Fig. 2). LTB<sub>4</sub> triggered an immediate  $[Ca^{2+}]_i$  spike that lasted only 6.5 ± 1.5 s, followed by a slow return to baseline  $[Ca^{2+}]_i$ , lasting a total of 33 ± 2.7 s. LTB<sub>4</sub> and uPAR cross-linking produced comparable peak increases in  $[Ca^{2+}]_i$ . Because the temporal configurations of the  $[Ca^{2+}]_i$  responses were so different, we also compared the areas under the curves of the  $[Ca^{2+}]_i$  tracings, referenced to the baseline  $[Ca^{2+}]_i$ , as a means of quantifying the overall magnitude of the increase in  $[Ca^{2+}]_i$ . This integrated  $[Ca^{2+}]_i$  signal induced by uPAR cross-

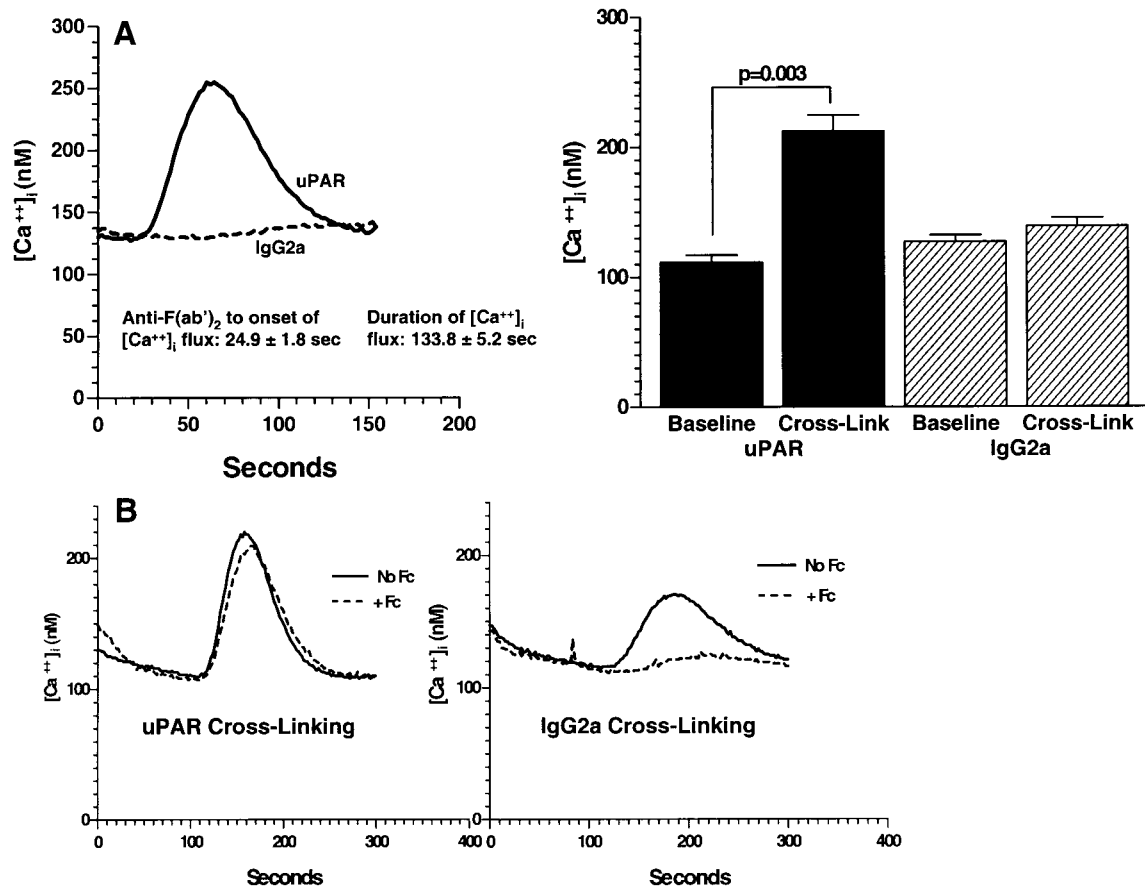


**FIGURE 1.** A, Left uPAR cross-linking triggers increased  $[Ca^{2+}]_i$ . Representative continuous tracings of  $[Ca^{2+}]_i$  over time after addition of goat anti-murine F(ab')<sub>2</sub> cross-linking Ab, demonstrating a gradual increase in  $[Ca^{2+}]_i$  after uPAR cross-linking, and no change in  $[Ca^{2+}]_i$  after cross-linking a control IgG2a. Right Pooled data show a significant difference between baseline and peak  $[Ca^{2+}]_i$  after uPAR cross-linking ( $n = 9$ ), but not after IgG2a cross-linking ( $n = 4$ ). B, Increased  $[Ca^{2+}]_i$  is not mediated by cross-linking FcR. uPAR cross-linking was performed with and without prior blockade of FcR, using purified murine Fc fragment. The presence of Fc blockade had no effect on the increase in  $[Ca^{2+}]_i$ . By contrast, cross-linking a control IgG2a induced a smaller increase in  $[Ca^{2+}]_i$ , and this was abrogated by Fc blockade.

linking was >10-fold the response elicited by LTB<sub>4</sub> ( $p < 0.0001$ ; Fig. 2).

#### Cross-linking uPAR triggers increased $[Ca^{2+}]_i$ in human monocytes

Human peripheral blood monocytes were subjected to uPAR cross-linking using a protocol very similar to that used for U937 cells. Based on preliminary experiments, the concentrations of Fc fragments and anti-uPAR mAb were adjusted (350 and 25  $\mu$ g/ml, respectively) to optimize the  $[Ca^{2+}]_i$  response and negate responses to the IgG2a control. As shown in Fig. 3, the baseline  $[Ca^{2+}]_i$  of monocytes was very similar to that of U937 cells, and uPAR cross-linking induced substantial increases in  $[Ca^{2+}]_i$  that exceeded the response of U937 cells and proceeded over essentially the same time frame. Control experiments confirmed that cross-linking the IgG2a control had no effect on  $[Ca^{2+}]_i$  (not shown). Thus, U937 cells appear to faithfully model the  $[Ca^{2+}]_i$  response induced by uPAR aggregation in authentic monocytes.

#### Mechanisms underlying $[Ca^{2+}]_i$ mobilization induced by uPAR cross-linking

Increased  $[Ca^{2+}]_i$  can be induced by mobilizing  $Ca^{2+}$  from intracellular stores such as the endoplasmic reticulum, or by  $Ca^{2+}$  influx across the plasma membrane (38). In many instances, mobilization of  $[Ca^{2+}]_i$  stores itself triggers a secondary influx of extracellular  $Ca^{2+}$  (38). The next series of experiments was per-

formed to ascertain the mechanisms by which uPAR cross-linking induces increased  $[Ca^{2+}]_i$ . U937 cells were treated with thapsigargin (5  $\mu$ M; Molecular Probes), for 30 min at 4°C to deplete  $[Ca^{2+}]_i$  stores (38, 39). Preliminary experiments confirmed that this pretreatment did not adversely affect cell viability (not shown). Thapsigargin pretreatment completely prevented any increase in  $[Ca^{2+}]_i$  in response to uPAR cross-linking (Fig. 4A). To examine the role of extracellular  $Ca^{2+}$ , EGTA (0.9 mM) was added to the incubation buffer immediately before adding the cross-linking Ab. Reducing the extracellular  $Ca^{2+}$  concentration from 1 to 0.1 mM only blunted the increase in  $[Ca^{2+}]_i$ . Preliminary experiments demonstrated that it was impossible to completely chelate extracellular  $Ca^{2+}$  with  $\geq 1$  mM EGTA without promptly reducing  $[Ca^{2+}]_i$  as well, usually below 50 nM. Nonetheless, the ability of thapsigargin to completely nullify the increase in  $[Ca^{2+}]_i$ , combined with the more modest reliance on extracellular  $Ca^{2+}$ , suggests that uPAR cross-linking initially triggers  $[Ca^{2+}]_i$  mobilization, which secondarily causes  $Ca^{2+}$  influx across the plasma membrane, amplifying and sustaining the overall increase in  $[Ca^{2+}]_i$ .

U937 cells were next pretreated with U73122 (5  $\mu$ M; Biomol, Plymouth Meeting, PA), an aminosteroid inhibitor of phospholipase C, or U73343, an inactive structural analogue, for 30 min at 4°C (40). Pretreating with U73122 significantly reduced the increase in  $[Ca^{2+}]_i$  induced by uPAR cross-linking, while the U73343 control had a small and statistically insignificant effect

**FIGURE 2.** LTB<sub>4</sub> stimulates increased [Ca<sup>2+</sup>]<sub>i</sub> in U937 cells. **A**, Results of a representative [Ca<sup>2+</sup>]<sub>i</sub> response to LTB<sub>4</sub> (100 nM) is shown, demonstrating a virtually immediate increase that was sustained for only 6.5 ± 1.5 s. **B**, The mean difference in [Ca<sup>2+</sup>]<sub>i</sub> from baseline to peak (Δ[Ca<sup>2+</sup>]<sub>i</sub>) is shown for LTB<sub>4</sub> (n = 5), compared with the response to uPAR cross-linking. While the Δ[Ca<sup>2+</sup>]<sub>i</sub> was comparable for the two modes of stimulation, the integrated Ca<sup>2+</sup> signal (area under the curve), as shown in **C**, was >10-fold higher for uPAR cross-linking.

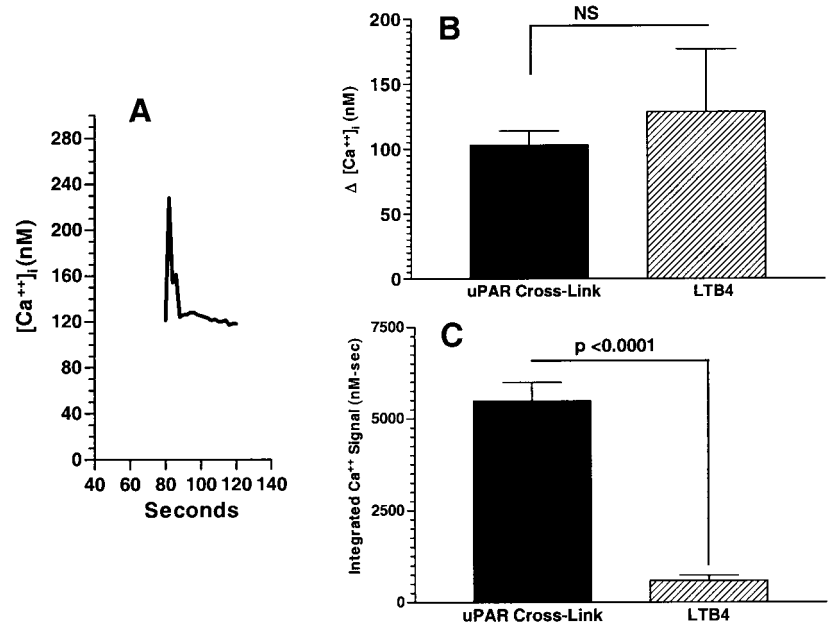


(Fig. 4B). Coupled with the previous results, this would suggest that uPAR cross-linking induces phospholipase C activation, generating Ins(1,4,5)P<sub>3</sub>, which in turn mobilizes Ca<sup>2+</sup> from Ins(1,4,5)P<sub>3</sub>-sensitive stores in the endoplasmic reticulum or other intracellular sites. To corroborate this interpretation, cellular levels of Ins(1,4,5)P<sub>3</sub> were measured after uPAR cross-linking (Fig. 5). Increased Ins(1,4,5)P<sub>3</sub> levels were noted promptly (within 10 s) after adding the goat anti-mouse F(ab')<sub>2</sub> Ab. Significantly increased Ins(1,4,5)P<sub>3</sub> levels were seen at 40 s and persisted through 120 s. Finally, experiments were performed to determine the effects of a TK inhibitor, herbimycin A. Herbimycin A completely abrogated Ca<sup>2+</sup> mobilization in response to uPAR cross-linking (Fig. 4B), indicating that this signaling pathway absolutely requires tyrosine phosphorylation. Preliminary experiments confirmed that treatments with U73122 and herbimycin A did not adversely affect cell viability (not shown). These results are consistent with TK-dependent activation of phospholipase C-γ1, but this interpretation remains speculative until subsequent studies are able to identify the targets for this TK activity (41, 42). Certainly, it is possible that other key targets of TK activity contribute indirectly to phospholipase C-γ1 activation by binding to its SH2 domains (42).

#### Role of ligand occupancy in uPAR-induced Ca<sup>2+</sup> mobilization

The first series of experiments was performed to determine the immediate effects of exposing cells to saturating concentrations of uPA. U937 cells were treated with 2000 or 4000 IU/ml (approximately 22–44 μg/ml), with minimal effect on [Ca<sup>2+</sup>]<sub>i</sub> (Fig. 6A). Because uPAR is present on the plasma membrane in both unoccupied and uPA-occupied forms and the anti-uPAR mAb used in the preceding experiments preferentially binds to unoccupied uPAR (37), we next sought to determine whether aggregation-induced Ca<sup>2+</sup> signaling differed between uPA-occupied vs unoccupied uPAR. To selectively cross-link occupied uPAR, the 3B10 Ab was substituted with an anti-uPA mAb, and the cross-linking protocol was otherwise duplicated. Cross-linking uPA significantly increased [Ca<sup>2+</sup>]<sub>i</sub>, although the magnitude of the response was roughly one-half of that induced by cross-linking the 3B10 mAb (Fig. 6B). Cells were pretreated with HMW-uPA (1 μg/ml) to occupy all available uPAR (27). Prior treatment with uPA had no effect on baseline [Ca<sup>2+</sup>]<sub>i</sub> levels, but doubled the magnitude of the Ca<sup>2+</sup> response to uPA cross-linking, effectively duplicating the response elicited by cross-linking uPAR directly (Fig. 6B). These

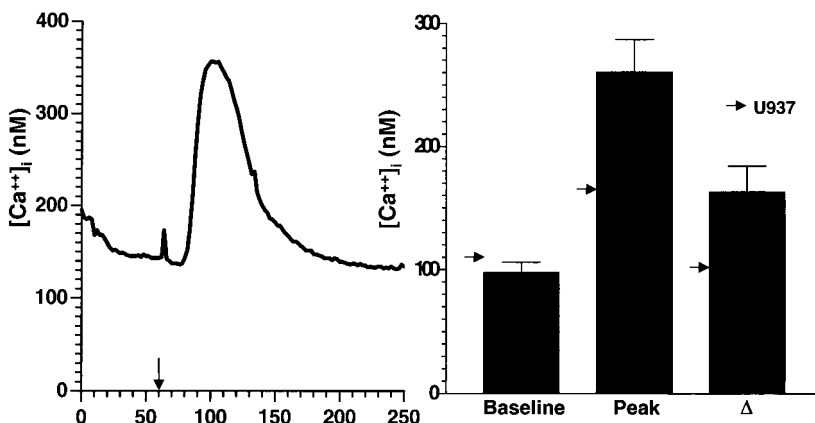


**FIGURE 3.** uPAR cross-linking increases [Ca<sup>2+</sup>]<sub>i</sub> in human monocytes. Freshly purified human peripheral blood monocytes were subjected to uPAR cross-linking. **A** representative experiment (*left*) shows the [Ca<sup>2+</sup>]<sub>i</sub> plotted over time after introduction of the cross-linking Ab (arrow). The pooled results of seven experiments, showing baseline, peak, and Δ[Ca<sup>2+</sup>]<sub>i</sub>, are shown on the *right* (mean ± SEM). The increase in [Ca<sup>2+</sup>]<sub>i</sub> began 15.6 ± 1.6 s after adding the cross-linking Ab, and lasted for 127.4 ± 11.2 s. Arrows indicate the comparable mean results obtained from U937 cells.

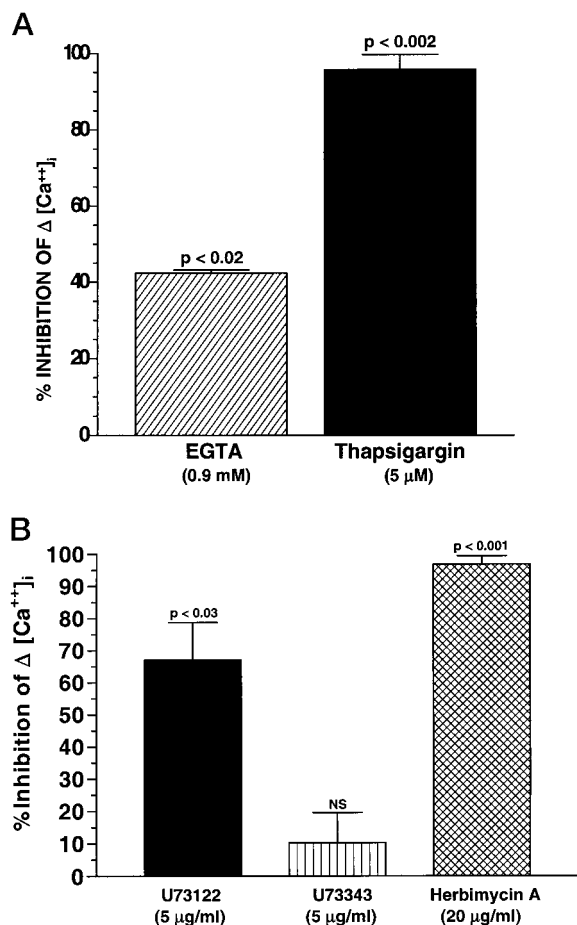


**FIGURE 4.** Mechanisms underlying increased  $[Ca^{2+}]_i$  in response to uPAR cross-linking. *A*, U937 cells treated with thapsigargin (5  $\mu$ M, 30 min at 4°C) to deplete  $[Ca^{2+}]_i$  stores demonstrated no increase in  $[Ca^{2+}]_i$  in response to uPAR cross-linking. By contrast, reducing extracellular  $[Ca^{2+}]$  by adding 0.9 mM EGTA only partially reduced  $[Ca^{2+}]_i$  response. *B*, Pretreatment with U73122 (5  $\mu$ M), a phospholipase C inhibitor, significantly reduced the  $\Delta [Ca^{2+}]_i$  in response to uPAR cross-linking, while U73343, an inactive structural analogue, had no significant effect. Herbimycin A (20  $\mu$ g/ml), a TK inhibitor, completely blocked any increase in  $[Ca^{2+}]_i$  in response to uPAR cross-linking. Data are expressed as percentage of inhibition of the  $\Delta [Ca^{2+}]_i$ , relative to untreated uPAR cross-linked controls (mean  $\pm$  SEM of three experiments).

results indicate that uPAR occupancy did not significantly influence the ability of uPAR cross-linking to trigger  $Ca^{2+}$  mobilization, at least within the extremes of occupancy with endogenously produced uPA (approximately 50%) and full receptor saturation.

#### Role of CR3 in uPAR-induced $Ca^{2+}$ mobilization

The bidirectional adapter functions shared by uPAR and CR3 have suggested that CR3 could serve the role of a signaling device for an otherwise signaling-deficient uPAR (5, 8). However, cross-linking other GPI-linked proteins can trigger signaling events, including increasing  $[Ca^{2+}]_i$  without defined cooperation with a transmembrane protein (43, 44). Therefore, experiments were performed to determine whether CR3 also serves an obligate role in the  $Ca^{2+}$  mobilization response to uPAR cross-linking. Additionally, previous studies have shown that cross-linking CR3 can itself induce  $[Ca^{2+}]_i$  mobilization (45, 46), so it was critical to demonstrate that cross-linking uPAR was not simply an indirect method for achieving CR3 aggregation. In the first series of experiments, U937 cells were subjected to cross-linking protocols

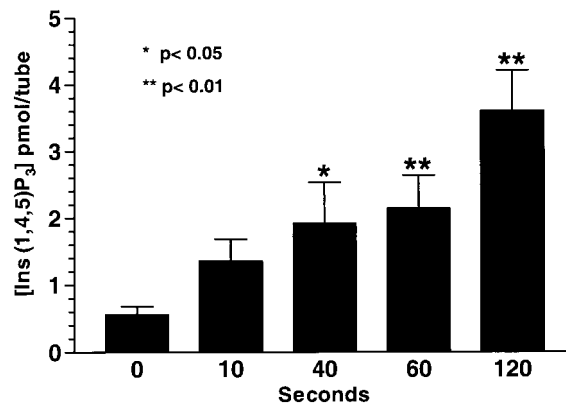


**FIGURE 5.** uPAR cross-linking induces a rapid increase in cellular Ins(1,4,5)P<sub>3</sub> levels. uPAR cross-linking was initiated in U937 cells, and perchloric acid extractions were performed at the indicated intervals after adding the cross-linking Ab. Cellular Ins(1,4,5)P<sub>3</sub> levels (pmol/tube), mean  $\pm$  SEM of four experiments are shown. Significant changes from control (0 s) are as indicated, using a Dunnett's test applied to a one-way ANOVA.

using Abs reactive to the CR3  $\alpha$ -chain (clone 44 and OKM1) and  $\beta$ -chain (TS1/18), all at 25  $\mu$ g/ml. The Fc fragment and the cross-linking mAb were used in identical fashion as for uPAR cross-linking. Cross-linking CR3 directly could not duplicate the effect of cross-linking uPAR (Fig. 7A). Cross-linking OKM1 mAb had no effect at all on  $[Ca^{2+}]_i$ , while cross-linking the 44 and TS1/18 mAbs produced small increases that were significantly less than the effect of uPAR cross-linking, measured in parallel. Given that the cross-linking protocols differed only by the choice of primary Ab, the  $[Ca^{2+}]_i$  transient elicited by uPAR cross-linking cannot be attributed to unintended cross-linking of any associated CR3. Finally, the ability of anti-CR3 mAbs to block uPAR-triggered  $Ca^{2+}$  mobilization was examined. The standard protocol for uPAR cross-linking could not be used, since the goat anti-murine F(ab')<sub>2</sub> Ab would also bind and aggregate the CR3 mAbs. Therefore, a biotinylated anti-uPAR mAb was used for these experiments. Fluo-3-AM-loaded U937 cells were first treated with the blocking Fc fragment, and biotinylated anti-uPAR (12.5  $\mu$ g/ml) and unlabeled anti-CR3 mAbs (25  $\mu$ g/ml) were added together for 30 min at 4°C. Streptavidin (0.04 U/ml) was then added to initiate cross-linking. Preliminary experiments confirmed that cross-linking biotinylated uPAR with streptavidin produced  $[Ca^{2+}]_i$  responses that were identical to those elicited by cross-linking unlabeled anti-uPAR mAb with the goat anti-F(ab')<sub>2</sub> Ab (not shown). None of the anti-CR3 mAbs had any inhibitory effect at all on the increase in  $[Ca^{2+}]_i$  in response to uPAR cross-linking (Fig. 7B), despite the fact that the same clone 44 anti-CR3  $\alpha$ -chain mAb completely blocked the CR3-dependent  $Ca^{2+}$  signal initiated by binding uPA to uPAR (8). These results suggest that aggregating uPAR can initiate activation signaling (i.e., increased  $[Ca^{2+}]_i$ ) independently of a cooperative function served by CR3.

#### Discussion

These studies demonstrate that aggregating uPAR can initiate intracellular signaling events in mononuclear phagocytes by mechanisms that differ in many respects from the pathways triggered by occupying uPAR with uPA. The increase in  $[Ca^{2+}]_i$  is similar in magnitude to the responses elicited by LTB<sub>4</sub> (Fig. 2). It is, nonetheless, difficult to draw valid comparisons between the  $[Ca^{2+}]_i$  responses to these stimuli. It is likely that uPAR aggregation, and consequently the increase in  $[Ca^{2+}]_i$ , is not synchronized in this

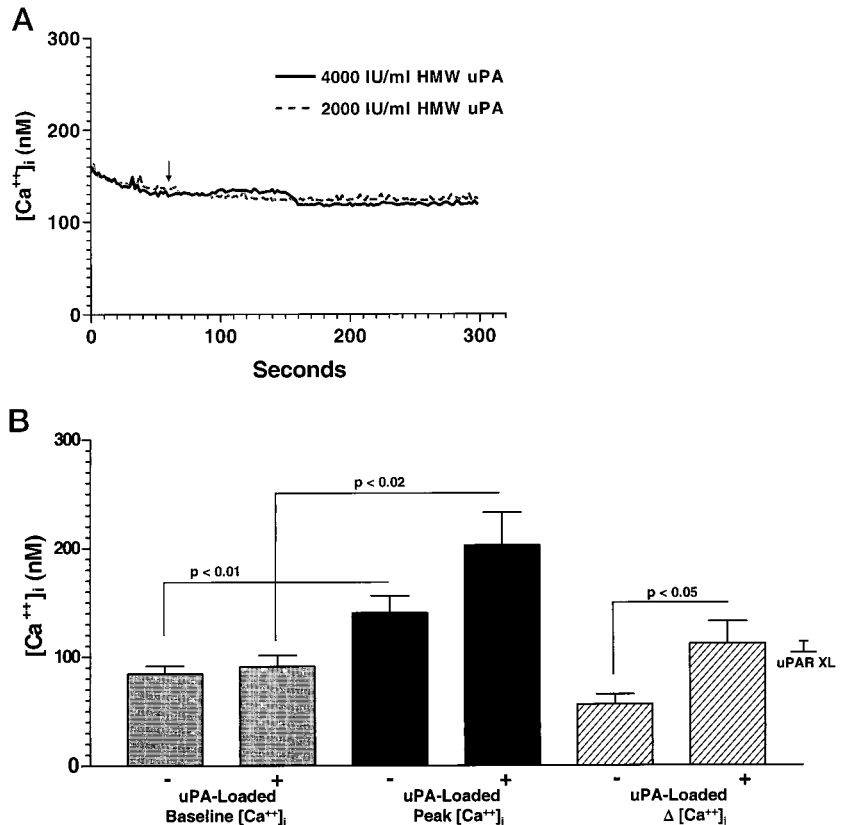


**FIGURE 6.** Role of uPA occupancy in uPAR-mediated  $\text{Ca}^{2+}$  mobilization. **A**, Representative tracing demonstrating that exposing U937 cells to 2000 or 4000 IU/ml of high m.w. uPA caused no acute change in  $[\text{Ca}^{2+}]_i$ . **B**, Occupied uPAR were selectively cross-linked (XL) by using an anti-uPA mAb. The baseline, peak, and  $\Delta[\text{Ca}^{2+}]_i$  (mean  $\pm$  SEM,  $n = 4$ ) are shown, both without (-) and with (+) pretreatment with high m.w. uPA (1  $\mu\text{g}/\text{ml}$ ). A significant increase in  $[\text{Ca}^{2+}]_i$  was seen in response to uPA cross-linking, but the  $\Delta[\text{Ca}^{2+}]_i$  was approximately one-half the response elicited by cross-linking with the anti-uPAR mAb (shown in Fig. 1). When cells were pretreated with uPA, the response to uPA cross-linking increased significantly ( $p < 0.05$ ), equaling the response to uPAR cross-linking.

population of cells, leading to a broadly distributed  $\text{Ca}^{2+}$  transient lasting for more than 2 min, whereas binding  $\text{LTB}_4$  to its receptors is more rapid and synchronous, yielding a brief  $\text{Ca}^{2+}$  transient. For this reason, we also examined the  $\Delta[\text{Ca}^{2+}]_i$  integrated over time to show that, in this respect, the response to uPAR cross-linking far exceeded the response to  $\text{LTB}_4$  (Fig. 2). Certainly, other factors such as the precise intracellular location of  $[\text{Ca}^{2+}]_i$  transients and the presence of  $[\text{Ca}^{2+}]_i$  oscillations also figure importantly in downstream activation signaling (38), but cannot be assessed by spectrofluorometry of cell suspensions. Artifacts of aggregation of FcR or CR3 during uPAR cross-linking was eliminated by demonstrating that FcR were effectively blocked (Fig. 1), and that cross-linking CR3  $\alpha$ - and  $\beta$ -chain Abs could not duplicate the effect of uPAR aggregation (Fig. 7A).

Aggregation of uPAR triggered the increase in  $[\text{Ca}^{2+}]_i$  through phospholipase C-dependent hydrolysis of membrane inositol phospholipids, yielding  $\text{Ins}(1,4,5)\text{P}_3$  and release of  $\text{Ca}^{2+}$  from  $\text{Ins}(1,4,5)\text{P}_3$ -sensitive intracellular stores, as demonstrated by the inhibitory effects of U73122, a phospholipase C inhibitor (Fig. 4B), the increase in cellular  $\text{Ins}(1,4,5)\text{P}_3$  levels (Fig. 5), and the inhibitory effects of thapsigargin, which depletes  $[\text{Ca}^{2+}]_i$  stores (Fig. 4A). The limited inhibitory effect of reducing available extracellular  $\text{Ca}^{2+}$  (Fig. 4A) suggests that  $\text{Ca}^{2+}$  entry through the plasma membrane is triggered secondarily after release of intracellular stores, but may amplify and sustain the increase in  $[\text{Ca}^{2+}]_i$ .

The original characterization of the uPAR protein stemmed from the search for uPA binding sites on the plasma membrane, and for this reason there has been an enduring bias that the principal physiologic function of uPAR revolves around its ability to bind uPA. However, further investigation has clearly established that uPAR serves several functions in adhesion, movement, and cellular signaling that are not mediated through associated uPA. uPAR is also a receptor for vitronectin (47) and high m.w. kinino-

gen (48). Monocyte and neutrophil chemotaxis requires uPAR in vitro, but this appears to be unrelated to associated uPA (4, 10). The ability of uPAR to facilitate CR3-dependent adhesion of monocytes to fibrinogen is actually reduced by uPA occupancy (5). Thus, one might expect that activation signaling through uPAR might likewise involve both uPA-dependent and uPA-independent mechanisms. To date, the role of uPAR in activation signaling has been approached largely by exposing cells to concentrations of uPA that would saturate available uPAR, or alternatively, dissociating uPA from uPAR and reconstituting uPA occupancy with lower concentrations of uPA. These approaches have demonstrated that uPA binding can trigger increased  $[\text{Ca}^{2+}]_i$ , and formation or activation of numerous signaling elements, including *src*- and *jak*-TKs, MAP kinases, diacylglycerol, *c-myc*, *c-fos*, *c-jun*, and Stat-1 (11–13, 16–21). The present study shows that major shifts in uPAR occupancy need not occur for uPAR to initiate activation signaling, since mobilization of  $[\text{Ca}^{2+}]_i$  by phosphoinositide hydrolysis is unaffected by partial vs complete uPA occupancy (Figs. 1 and 6). Moreover, uPAR aggregation at cell-substratum interfaces, focal adhesions, and at the leading edge of migrating cells is well documented, providing a natural physiologic counterpart for experimental uPAR cross-linking (4, 5, 29–31, 49). This is certainly not to say that uPA occupancy should assume secondary importance in uPAR signaling pathways. Signaling events initiated by uPA binding or catalytic activity may be sufficiently distinct from those initiated by uPAR aggregation that the pathways may be complementary in leukocyte activation.

The formation of lateral associations between uPAR and  $\beta_2$  integrins is highly dynamic and reversible. In nonpolarized neutrophils, uPAR associates closely with CR3, but as the cells polarize, uPAR and CR4 (CD11c/CD18) colocalize to lamellopodia, while CR3 segregates to the uropod (31, 49). The increase in  $[\text{Ca}^{2+}]_i$

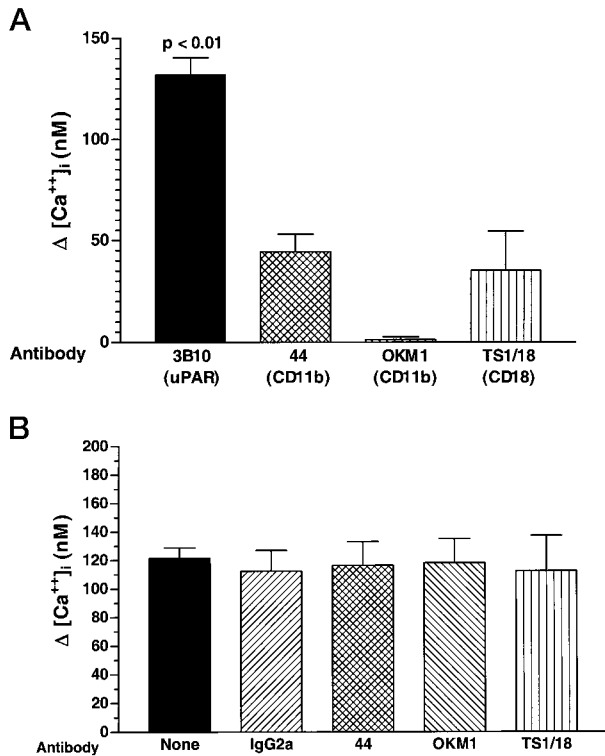


**FIGURE 7.** Role of CR3 (CD11b/CD18) in uPAR-induced  $\text{Ca}^{2+}$  mobilization. **A**, Cross-linking three different mAbs reactive to CR3 (clones 44 and OKM1, reactive to the  $\alpha$ -chain, and TS1/18, reactive to the  $\beta$ -chain) of U937 cells produced  $\Delta[\text{Ca}^{2+}]_i$  that were significantly smaller than the response to uPAR cross-linking. Data shown are mean  $\pm$  SEM for  $n = 5$  (uPAR Ab),  $n = 4$  (clone 44),  $n = 3$  (OKM1 and TS1/18) comparing all CR3 Abs to uPAR Ab, using Dunnett's multiple comparison test applied to a one-way ANOVA. **B**, Anti-CR3 mAbs do not block uPAR-induced  $[\text{Ca}^{2+}]_i$  mobilization. U937 cells were pretreated with 25  $\mu\text{g}/\text{ml}$  of Abs as shown, concurrently with 12.5  $\mu\text{g}/\text{ml}$  biotinylated anti-uPAR mAb, and uPAR was subsequently cross-linked with streptavidin. The  $\Delta[\text{Ca}^{2+}]_i$  in response to uPAR cross-linking was unaffected by the presence of any CR3 mAbs (mean  $\pm$  SEM,  $n = 3$ ).

triggered by uPA in neutrophils requires a close association between uPAR and CR3 (8). The present study demonstrates that uPAR can participate in activation signaling even when its association with CR3 is disrupted. The combination of CR3-dependent and CR3-independent signaling pathways certainly expands the potential versatility of uPAR in leukocyte activation signaling.

One of the major questions as yet unresolved is how leukocyte uPAR becomes aggregated *in vivo*. This might occur by any of several mechanisms. uPAR may aggregate as cells adhere to surfaces coated with a uPAR counterligand such as vitronectin (6, 47, 50, 51). Similarly, uPAR may aggregate as they form complexes with CR3 or other integrins, and are drawn into a clustered orientation as the integrins adhere to their counterligands (5, 15, 47). Occupancy with uPA may actually play a similar role in promoting uPAR aggregation, since uPA-occupied uPAR can segregate from unoccupied uPAR and concentrate at focal adhesions and cell-cell contacts (30) and binding uPA to uPAR can polarize the distribution of uPAR in preadherent U937 cells (52). Finally, uPAR may cluster in caveolae or similar detergent-insoluble domains of the plasma membrane (13, 53). These regions are rich in GPI-linked receptors and signal transduction molecules, so it is possible that changes in the distribution or composition of these domains could cause uPAR to accumulate in these regions in close proximity to signal transducers (54).

In summary, we have shown that aggregation of uPAR (CD87) in mononuclear phagocytes can trigger  $[\text{Ca}^{2+}]_i$  mobilization by phospholipase C-mediated phosphoinositide hydrolysis and formation of  $\text{Ins}(1,4,5)\text{P}_3$ . This is distinct from previously described pathways of uPAR-mediated signaling in leukocytes, in that it does not require changes in receptor occupancy with uPA or complex formation with CR3. Thus, uPAR aggregation may provide a mechanistic link between adhesion, directional migration, and activation signaling in leukocytes entering sites of inflammation.

## Acknowledgments

We thank Donna Harsh for assistance with spectrofluorometry and Ikuko Mizukami and Laura Mayo-Bond for preparation of anti-uPAR Ab.

## References

- Schleiffenbaum, B., and J. Fehr. 1996. Regulation and selectivity of leukocyte emigration. *J. Lab. Clin. Med.* 127:151.
- Andreasen, P. A., L. Kjoller, L. Christensen, and M. J. Duffy. 1997. The urokinase-type plasminogen activator system in cancer metastasis: a review. *Int. J. Cancer* 72:1.
- Blasi, F. 1997. uPA, uPAR, PAI-1: key intersection of proteolytic, adhesive and chemotactic highways? *Immunol. Today* 18:415.
- Gyetko, M., R. Todd III, C. Wilkinson, and R. Sitrin. 1994. The urokinase receptor is required for monocyte chemotaxis *in vitro*. *J. Clin. Invest.* 93:1380.
- Sitrin, R., R. Todd, H. Petty, T. Brock, S. Shollenberger, E. Albrecht, and M. Gyetko. 1996. The urokinase receptor (CD87) facilitates CD11b/CD18-mediated adhesion of human monocytes. *J. Clin. Invest.* 97:1942.
- Wei, Y., M. Lukashev, D. Simon, S. Bodary, S. Rosenberg, M. Doyle, and H. Chapman. 1996. Regulation of integrin function by the urokinase receptor. *Science* 273:1551.
- May, A. E., S. M. Kanse, L. R. Lund, R. H. Gisler, B. A. Imhof, and K. T. Preissner. 1998. Urokinase receptor (CD87) regulates leukocyte recruitment via  $\beta_2$  integrins *in vivo*. *J. Exp. Med.* 188:1029.
- Cao, D., I. Mizukami, B. Garni-Wagner, A. Kindzelskii, R. Todd, L. Boxer, and H. Petty. 1995. Human urokinase-type plasminogen activator primes neutrophils for superoxide anion release: possible roles of complement receptor type III and calcium. *J. Immunol.* 154:1817.
- Kirchheimer, J. C., and H. G. Remold. 1989. Endogenous receptor-bound urokinase mediates tissue invasion of human monocytes. *J. Immunol.* 143:2634.
- Gyetko, M., R. Sitrin, J. Fuller, R. Todd, and T. Standiford. 1995. Function of the urokinase receptor (CD87) in PMN chemotaxis. *J. Leukocyte Biol.* 58:533.
- Bohuslav, J., V. Horejsi, C. Hansmann, J. Stöckl, U. Weidle, O. Majdic, I. Barke, W. Knapp, and H. Stockinger. 1995. Urokinase plasminogen activator receptor,  $\beta_2$  integrins, and *src*-kinases within a single receptor complex of human monocytes. *J. Exp. Med.* 181:1381.
- Dumler, I., A. Weis, O. A. Mayboroda, C. Maasch, U. Jerke, H. Haller, and D. C. Gulba. 1998. The Jak/Stat pathway and urokinase receptor signaling in human aortic vascular smooth muscle cells. *J. Biol. Chem.* 273:315.
- Koshelnick, Y., M. Ehart, P. Hufnagl, P. C. Heinrich, and B. R. Binder. 1997. Urokinase receptor is associated with the components of the JAK1/STAT1 signaling pathway and leads to activation of this pathway upon receptor clustering in the human kidney epithelial tumor cell line TCL-598. *J. Biol. Chem.* 272:28563.
- Xue, W., A. Kindzelskii, R. Todd, and H. Petty. 1994. Physical association of complement receptor type 3 and urokinase-type plasminogen activator receptor in neutrophil membranes. *J. Immunol.* 152:4630.
- Ciambone, G., and P. McKeown-Longos. 1992. Vitronectin regulates the synthesis and localization of urokinase-type plasminogen activator in HT-1080 cells. *J. Biol. Chem.* 267:13617.
- Del Rosso, M., E. Anichini, N. Pedersen, F. Blasi, G. Fibbi, M. Pucci, and M. Ruggiero. 1993. Urokinase-urokinase receptor interaction: non-mitogenic signal transduction in human epidermal cells. *Biochem. Biophys. Res. Commun.* 190:347.
- Anichini, E., G. Fibbi, M. Pucci, R. Caldini, M. Chevanne, and M. DelRosso. 1994. Production of second messengers following chemotactic and mitogenic urokinase-receptor interaction in human fibroblasts and mouse fibroblasts transfected with human urokinase receptor. *Exp. Cell Res.* 213:438.
- Anichini, E., A. Zamperini, M. Chevanne, R. Caldini, M. Pucci, G. Fibbi, and M. Del Rosso. 1997. Interaction of urokinase-type plasminogen activator with its receptor rapidly induces activation of glucose transporters. *Biochemistry* 36:3076.
- Rabbani, S. A., J. Gladu, A. P. Mazar, J. Henkin, and D. Goltzman. 1997. Induction in human osteoblastic cells (SaOS2) of the early response genes *fos*, *jun*, and *myc* by the amino terminal fragment (ATF) of urokinase. *J. Cell. Physiol.* 172:137.
- Nguyen, D. H., I. M. Hussaini, and S. L. Gonias. 1998. Binding of urokinase-type plasminogen activator to its receptor in MCF-7 cells activates extracellular signal-regulated kinase 1 and 2 which is required for increased cellular motility. *J. Biol. Chem.* 273:8502.
- Tang, H., D. M. Kerins, Q. Hao, T. Inagami, and D. E. Vaughan. 1998. The urokinase-type plasminogen activator receptor mediates tyrosine phosphorylation



- of focal adhesion proteins and activation of mitogen-activated protein kinase in cultured endothelial cells. *J. Biol. Chem.* 273:18268.
22. Resnati, M., M. Guttinger, S. Valcamonica, N. Sidenius, F. Blasi, and F. Fazioli. 1996. Proteolytic cleavage of the urokinase receptor substitutes for the agonist-induced chemotactic effect. *EMBO J.* 15:1572.
  23. Shetty, S., A. Kumar, A. R. Johnson, and S. Idell. 1995. Regulation of mesothelial cell mitogenesis by antisense oligonucleotides for the urokinase receptor. *Antisense Res. Dev.* 5:307.
  24. Rabbani, S. A., A. P. Mazar, S. M. Bernier, M. Haq, I. Bolivar, J. Henkin, and D. Goltzman. 1992. Structural requirements for the growth factor activity of the amino-terminal domain of urokinase. *J. Biol. Chem.* 267:14151.
  25. Ploug, M., E. Rønne, N. Behrendt, A. Jensen, F. Blasi, and K. Danø. 1991. Cellular receptor for urokinase plasminogen activator: carboxy-terminal processing and membrane anchoring by glycosyl-phosphatidylinositol. *J. Biol. Chem.* 266:1926.
  26. Kirchheimer, J. C., Y. H. Nong, and H. G. Remold. 1988. IFN- $\gamma$ , tumor necrosis factor- $\alpha$ , and urokinase regulate the expression of urokinase receptors on human monocytes. *J. Immunol.* 141:4229.
  27. Sitrin, R., R. Todd III, I. Mizukami, T. Gross, S. Shollenberger, and M. Gyetko. 1994. Cytokine specific regulation of urokinase receptor (CD87) expression by U937 mononuclear phagocytes. *Blood* 84:1268.
  28. Plesner, T., M. Ploug, V. Ellis, E. Rønne, G. Høyer-Hansen, M. Wittrup, T. Linhardt-Pedersen, T. Tscherning, K. Danø, and N. Ebbe-Hansen. 1994. The receptor for urokinase-type plasminogen activator and urokinase is translocated from two distinct intracellular compartments to the plasma membrane on stimulation of human neutrophils. *Blood* 83:808.
  29. Estreicher, A., J. Muhlhauser, J. Carpentier, L. Orci, and J. Vassalli. 1990. The receptor for urokinase type plasminogen activator polarizes expression of the protease to the leading edge of migrating monocytes and promotes degradation of enzyme inhibitor complexes. *J. Cell Biol.* 111:783.
  30. Myohanen, H. T., R. W. Stephens, K. Hedman, H. Tapiovaara, E. Rønne, G. Hoyer-Hansen, K. Dano, and A. Vaheri. 1993. Distribution and lateral mobility of the urokinase-receptor complex at the cell surface. *J. Histochem. Cytochem.* 41:1291.
  31. Kindzelskii, A. L., Z. O. Laska, R. F. Todd III, and H. R. Petty. 1996. Urokinase-type plasminogen activator receptor reversibly dissociates from complement receptor type 3 ( $\alpha$ M  $\beta$ 2' CD11b/CD18) during neutrophil polarization. *J. Immunol.* 156:297.
  32. Min, H., R. Semnani, I. Mizukami, K. Watt, R. Todd III, and D. Liu. 1992. cDNA for Mo3, a monocyte activation antigen, encodes the human receptor for urokinase plasminogen activator. *J. Immunol.* 148:3636.
  33. Dana, N., B. Styrt, J. D. Griffin, R. F. Todd III, M. S. Klempner, and M. A. Arnaout. 1986. Two functional domains in the phagocyte membrane glycoprotein Mo1 identified with monoclonal antibodies. *J. Immunol.* 137:3259.
  34. Sanchez-Madrid, F., J. Nagy, E. Robbins, P. Simon, and T. Springer. 1983. A human leukocyte differentiation antigen family with distinct  $\alpha$  subunits and a common  $\beta$  subunit: the lymphocyte function-associated antigen (LFA-1), the C3bi complement receptor (OKM-1/Mac-1), and the p150,95 molecule. *J. Exp. Med.* 158:1785.
  35. Gryniewicz, G., M. Poenie, and R. Y. Tsien. 1985. A new generation of  $\text{Ca}^{2+}$  indicators with greatly improved fluorescence properties. *J. Biol. Chem.* 260:3440.
  36. Merritt, J. E., S. A. McCarthy, M. P. Davies, and K. E. Moores. 1990. Use of fluo-3 to measure cytosolic  $\text{Ca}^{2+}$  in platelets and neutrophils: loading cells with the dye, calibration of traces, measurements in the presence of plasma, and buffering of cytosolic  $\text{Ca}^{2+}$ . *Biochem. J.* 269:513.
  37. Mizukami, I., B. Garni-Wagner, L. deAngelo, M. Liebert, A. Flint, D. Lawrence, R. Cohen, and R. Todd. 1994. Immunologic detection of the cellular receptor for urokinase plasminogen activator. *Clin. Immunol. Immunopathol.* 71:96.
  38. Putney, J. W. Jr., and G. S. Bird. 1993. The inositol phosphate-calcium signaling system in nonexcitable cells. *Endocr. Rev.* 14:610.
  39. Treiman, M., C. Caspersen, and S. B. Christensen. 1998. A tool coming of age: thapsigargin as an inhibitor of sarco-endoplasmic reticulum  $\text{Ca}^{2+}$ -ATPases. *Trends Pharmacol. Sci.* 19:131.
  40. Smith, R. J., L. M. Sam, J. M. Justen, G. L. Bundy, G. A. Bala, and J. E. Bleasdale. 1990. Receptor-coupled signal transduction in human polymorphonuclear neutrophils: effects of a novel inhibitor of phospholipase C-dependent processes on cell responsiveness. *J. Pharmacol. Exp. Ther.* 253:688.
  41. Rhee, S. G., and Y. S. Bae. 1997. Regulation of phosphoinositide-specific phospholipase C isozymes. *J. Biol. Chem.* 272:15045.
  42. Kamat, A., and G. Carpenter. 1997. Phospholipase C- $\gamma$ 1: regulation of enzyme function and role in growth factor-dependent signal transduction. *Cytokine Growth Factor Rev.* 8:109.
  43. Pugin, J., V. V. Kravchenko, J. D. Lee, L. Kline, R. J. Ulevitch, and P. S. Tobias. 1998. Cell activation mediated by glycosylphosphatidylinositol-anchored or transmembrane forms of CD14. *Infect. Immun.* 66:1174.
  44. Stefanova, I., V. Horejsi, I. Ansotegui, W. Knapp, and H. Stockinger. 1991. GPI-anchored cell-surface molecules complexed to protein tyrosine kinases. *Science* 254:1016.
  45. Altieri, D. C., S. J. Starnes, and C. G. Gahmberg. 1992. Regulated  $\text{Ca}^{2+}$  signaling through leukocyte CD11b/CD18 integrin. *Biochem. J.* 288:465.
  46. Walzog, B., R. Seifert, A. Zakrzewicz, P. Gaeltgens, and K. Ley. 1994. Cross-linking of CD18 in human neutrophils induces an increase of intracellular free  $\text{Ca}^{2+}$ , exocytosis of azurophilic granules, quantitative up-regulation of CD18, shedding of L-selectin, and actin polymerization. *J. Leukocyte Biol.* 56:625.
  47. Wei, Y., D. Waltz, N. Rao, R. Drummond, S. Rosenberg, and H. Chapman. 1994. Identification of the urokinase receptor as an adhesion receptor for vitronectin. *J. Biol. Chem.* 269:32380.
  48. Colman, R. W., R. A. Pixley, S. Najamunnisa, W. Yan, J. Wang, A. Mazar, and K. R. McCrae. 1997. Binding of high molecular weight kininogen to human endothelial cells is mediated via a site within domains 2 and 3 of the urokinase receptor. *J. Clin. Invest.* 100:1481.
  49. Kindzelskii, A. L., M. M. Eszes, R. F. Todd III, and H. R. Petty. 1997. Proximity oscillations of complement type 4 ( $\alpha$ X  $\beta$ 2) and urokinase receptors on migrating neutrophils. *Biophys. J.* 73:1777.
  50. Ciambone, G., and P. McKeown-Longo. 1990. Plasminogen activator inhibitor type 1 stabilizes vitronectin-dependent adhesions in HT-1080 cells. *J. Cell Biol.* 111:2183.
  51. Waltz, D., and H. Chapman. 1994. Reversible cellular adhesion to vitronectin linked to urokinase receptor occupancy. *J. Biol. Chem.* 269:14746.
  52. Franco, P., C. Iaccarino, F. Chiaradonna, A. Brandazza, C. Iavarone, M. R. Mastronicola, M. L. Nolli, and M. P. Stoppelli. 1997. Phosphorylation of human pro-urokinase on Ser138/303 impairs its receptor-dependent ability to promote myelomonocytic adherence and motility. *J. Cell Biol.* 137:779.
  53. Stahl, A., and B. M. Mueller. 1995. The urokinase-type plasminogen activator receptor, a GPI-linked protein, is localized in caveolae. *J. Cell Biol.* 129:335.
  54. Shaul, P. W., and R. G. Anderson. 1998. Role of plasmalemmal caveolae in signal transduction. *Am. J. Physiol.* 275:L843.